How to design a zero-degradation battery: compensating for loss of lithium inventory in LFP cells with LFO additives

Sunil Kumar Rawat*, Monica Marinescu, Gregory James Offer, Simon E. J. O'Kane, Ruihe Li

*Corresponding author:
E-mail address: s.rawat@imperial.ac.uk

Affiliations:
Department of Mechanical Engineering,
Electrochemical Science and Engineering Group
Imperial College London

Abstract

Loss of lithium inventory (LLI) caused by side reactions in lithium-ion cells is one of the major reasons behind their capacity fade and shorter cycle life. Research in academia and industry has explored additives such as Lithium Iron oxide (Li_5FeO_4) in LFP-based battery chemistries that sacrifice their lithium inventory to compensate for LLI. Over the last ~15 years, research has proven that LFO can compensate for LLI and help maintain stable cell performance, and more recently, CATL & Rimac announced its commercial-level usage claiming to have achieved zero degradation for extended periods. However, the specifics behind achieving such excellent performance are neither fully disclosed by them nor much explored in the literature.

This work advances and broadens the existing theoretical understanding of employing sacrificing agents and demonstrates how exactly LFO can be employed in commercial large LFP cells with LFP/LFO positive electrode (PE) and Graphite negative electrode (NE) using simulations run by building a full-cell physics-based model in PyBaMM. The work digs deeper into the science behind releasing lithium inventory from LFO, and its impact on cell degradation, discharge capacity, and cell life. The work also attempts to find the optimal methods to control lithium release from LFO and the optimum weight fraction of LFO to minimize cell degradation and achieve long-lasting, zero-degradation batteries. Model results reveal that the slow lithium release maintains the cell balancing and keeps the degradation rates of SEI formation and lithium plating under control, while rapid lithium release and excessive LFO content can accelerate their degradation rates resulting in faster pore-clogging in the NE and lower cycle life. This work shows that merely adding lithium-rich additives does not promise high-performance batteries; instead depends on using them in optimal amounts and ensuring the controlled release of lithium inventory through appropriate control methods.

Main

Loss of lithium inventory (LLI) is one of the major reasons behind the capacity fade and reduced life cycle in lithium-ion batteries (Birkl et al., 2017), (Edge et al., 2021). The formation of SEI along with other degradation mechanisms in lithium-ion cells leads to the consumption of lithium ions and hence LLI (Edge et al., 2021). LLI becomes even more intense during formation & first few operation cycles because of accelerated SEI growth. Recent breakthroughs in research and industry have explored how LLI could be compensated using an additive that sacrifices its lithium inventory for consumption by SEI and other degradation mechanisms, thus improving battery efficiency and longevity. Lithium Iron oxide (Li_5FeO_4) is seen as an excellent candidate for its use as an additive for LFP-based battery chemistries (Johnson et al., 2010), (Su et al., 2016), (Liu et al., 2024). The antifluorite structure of LFO helps it to store as much as 4 times more lithium ions (Johnson et al., 2010) as compared to standard LFP cathodes helping it to achieve very high theoretical & practical charge per gram of active material (Dose et al., 2018) (Liu et al., 2024).

However, the stored lithium ion in LFO is released permanently in two stages—at open circuit potential of 3.5 V and 4.0 V—when the cell is overcharged (Johnson et al., 2010), (Liu et al., 2024), making it traditionally suitable only for primary cells. However, in a secondary cell, the lithium released can be used to compensate for LLI (Johnson et al., 2010), (Su et al., 2016), (Dose et al., 2018), (Liu et al., 2024). The use of LFO as a sacrificing agent at the lab scale shows that LFO can compensate for LLI during formation & charge-discharge cycles and help maintain stable cell performance. Companies like CATL & Rimac have recently demonstrated the commercial viability of LFO as a sacrificing agent (Pathirana, 2024), (Murray, 2024). CATL showed that LFO can be implemented as a cathode additive in LFP batteries to achieve zero degradation for the first 1000 cycles (Pathirana, 2024) . They focused on lithium release from LFO in the early phase of battery life. Rimac Energy's approach is slightly different as they hinted towards gradual lithium release from LFO and claimed to have achieved zero capacity fade for two years (Murray, 2024). Rimac has also mentioned having used an advanced power conversion system to achieve such performance (Murray, 2024). Neither of the two companies has disclosed the exact methods, leaving researchers speculating on the underly principles, mechanisms, and methods of employing LFO as an additive in commercial cells. Commercial-level usage of LFO and understanding of it are also missing in the literature. Using the above innovations as motivation our work offers deeper insights into how exactly LFO can be employed in commercial LFP cells with LFP/LFO positive electrode (PE) and Graphite negative electrode (NE) using simulations run by building a full-cell physics-based model in PyBaMM.

The work digs deeper into the science behind releasing lithium inventory from LFO, its impact on cell degradation (SEI, lithium plating), discharge capacity, and cell life. The work also attempts to find the optimal methods to control lithium release from LFO and the optimum weight fraction of LFO to minimize cell degradation and achieve long-lasting, zero-degradation batteries. Work concludes that (a) the release of lithium inventory from additives can be controlled to maximize the benefits of their usage instead of releasing all their lithium inventory at once, (b) controlled slow lithium release maintains the cell balancing and reduces the degradation rates, while rapid lithium release can accelerate cell degradation (c) using optimum weight fraction of LFO is crucial for minimizing cell degradation as excess LFO even though appears beneficial because of its capability to provide more lithium inventory and higher usable cell capacity but is counterproductive as it promotes faster cell degradation resulting in shorter cycle life of the cell. Hence, this study advances and broadens the existing theoretical understanding of employing sacrificing agents, such as LFO, in commercial lithium-ion cells. Additionally, we conclude that merely adding lithium-rich additives does not promise high-performance batteries; instead depends on using them in optimal amounts and ensuring the controlled release of lithium inventory through appropriate control methods.

The mechanism of lithium release is discussed in Section 1, and its impact on degradation, cell capacity, and cell life is discussed in Section 2. Attempts to find optimal methods to control lithium release from LFO and optimal weight fraction of LFO to achieve greater cell performance can be found in Section 3 and Section 4, respectively. The methods section explains the implementation of the work in PyBaMM, which contains a discussion on how the model is set up, what assumptions are made, how the virtual experiments are set, and how the various methods of controlling lithium release from LFO are set up. The conclusion section summarises the important results from the current work and its impact and potential future work.

Section 1: Theoretical mechanism of lithium release from LFO and a PyBaMM simulation to understand it better

LFO (Li_5FeO_4) material as a sacrificing agent in lithium-ion cells releases its lithium inventory by following the below two reactions:

$$Li_5FeO_4 \rightarrow Li_3FeO_{3.5} + 0.25O_2\uparrow + 2Li^+ + 2e^- \qquad [1]$$

$$Li_3FeO_{3.5} \rightarrow LiFeO_2 + 0.75O_2\uparrow + 2Li^+ + 2e^- \qquad [2]$$

The first irreversible release of lithium-ion happens when the half-cell open circuit potential (OCP) of LFO material is around 3.5 V (reaction [1]) and the second irreversible lithium release happens at OCP of 4.0 V (reaction [2]) (Liu et al., 2024). Figure 1 shows the half-cell OCP of a pure LFO material (Liu et al., 2024) vs stoichiometry. The two relative plateaus at around 3.5 V and 4.0 V of the LFO OCP curve correspond to the lithium release from LFO as per the abovementioned reactions (reaction [1] & reaction [2]) (Liu et al., 2024). From the above reactions and Figure 1, it can be inferred that as the LFO (Li_5FeO_4) releases its lithium irreversibly, the permanent LFO de-lithiation (which means permanent lithium loss from LFO) shifts the stoichiometry of LFO slowly from 1 (fully lithiated i.e. Li_5FeO_4) to 0 (completed depleted $LiFeO_2$) and its OCP from 2.5 V to 4.5 V (Liu et al., 2024). It is important to again highlight that the shift in stoichiometry and the corresponding change in OCP is permanent in LFO material. This means that as LFO releases its lithium inventory, it shifts to a lower stoichiometry value or a higher OCP value permanently. The stoichiometry and the OCP of the material stay at this value unless more lithium is released from it.

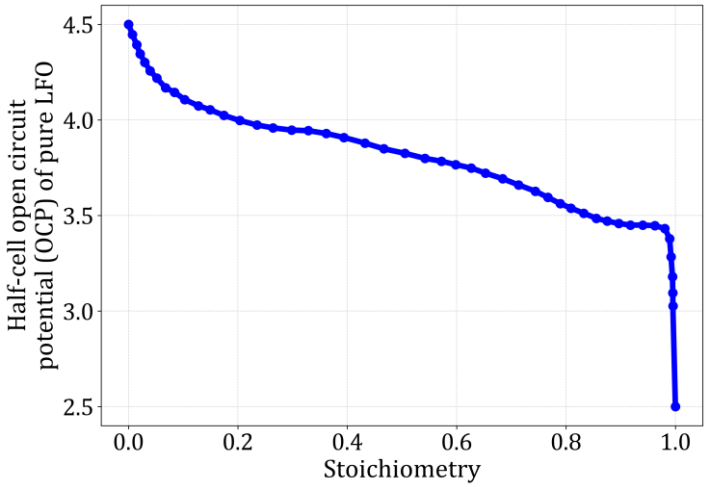

Figure 1: Half-cell open circuit potential (OCP) of a pure LFO material vs stoichiometry (Liu et al., 2024, Sepideh, 2017)

From the above reactions and Figure 1, It can also be inferred that when the LFO material is used as a sacrificing agent/secondary phase in PE in a lithium-ion cell, the cell must be charged to voltages such that the OCP of LFO at least crosses 3.5 V. This ensures that the reaction [1] is activated and release of lithium from LFO material happens. Figure 1 also shows that the upper limit of OCP of LFO material is around 4.5 V. This means that the LFO material and its full capacity to release lithium inventory is utilized only when the cell level voltage limit for charging is kept as high as 4.5 V. Such high charging voltage limits ensures that the half-cell OCP of around 4.5 V is achieved for LFO material (as NE OCP is close to zero during such charging limits) (include reference) and the release of lithium from LFO can happen.

Hence, it can be concluded that the cell level charging voltage limits should be kept such that both the plateaus at 3.5 V and 4.0 V are accessed on the LFO OCP curve. This ensures the LFO material is fully utilized, leading to the release of extra lithium-ions and, hence, increased lithium inventory in the cells. The availability of the extra lithium then compensates for lithium lost due to side reactions.

To better understand the lithium release from LFO, and the corresponding variation in its OCP and to explore more on the inferences made from Figure 1 and Reactions [1] and [2], a PyBaMM simulation is done to mimic the real-life usage of LFO in commercial LFP cells. This is done by setting up a simulation case called *'Case 1'*. A detailed discussion on setting up a simulation Case 1 can be found in parts 1, part2, and part 3 of the methods section of this paper. In summary, the simulation case is set up by considering the virtual lithium-ion cell with LFP/LFO-based composite PE and Graphite NE. Composite PE has an LFO weight equivalent

to 4% of the LFP weight. LFP is referred to as the primary phase PE, and LFO is referred to as the secondary phase PE. The simulation experiment is done on the virtual cell where a cell is made to cycle for 1000 charge-discharge aging cycles (the cell undergoes the repetition of 25 normal charge-discharge cycles followed by an overcharge cycle and a rapid performance test) whose details are discussed in part 2 of the methods section. The charging cell voltage limit for 25 normal charge cycles and an overcharge cycle is kept in the range of 2.5 V to 3.6 V and 2.5 V to 4.5 V, respectively. As discussed previously, overcharging is done to ensure that the full potential of LFO material is utilized. More details on the number of normal charges and overcharges that the cell undergoes are discussed in part 3 (case 1) of the methods section.

Figure 2, obtained from simulation Case 1, shows the lithium release from LFO material ('Total lithium in secondary phase in positive electrode [mol]') and the corresponding change in its OCP ('X-averaged positive electrode secondary open-circuit potential [V]') vs cell throughput capacity [A-h] for first six overcharges only. During the first 25 normal charging-discharging cycles (up to a throughput capacity of 4800 Ah) with cell voltage in the range of 2.5 V to 3.6 V, the release of lithium moles from LFO follows the parabolic curve. This means that during the normal charge with an upper voltage limit of 3.6 V, some part of the OCP curve of the LFO active material is still active and accessible (plateau at 3.5 V is accessible on the LFO OCP curve) leading to some lithium release into the system. During each overcharge (indicated by the six steps decrease in lithium moles of LFO), charging is done until the cell voltage reaches 4.5 V and then the voltage is held at 4.5 V. In this process, the OCP of LFO reaches a value as high as 4.5 V and total lithium moles in LFO material drop sharply. This means that LFO material is significantly activated (both the plateaus at 3.5 V and 4.0 V are accessed on the LFO OCP curve) during overcharge and more lithium moles are released from LFO material leading to a sharp drop in available lithium moles. The released lithium moles become the part of total lithium inventory in the cell. The first thing to note from Figure 2 is that whenever the lithium moles from LFO are released, it leads to an increase in its OCP, and as discussed previously, this is because the lithium release from LFO material is irreversible (Liu et al., 2024), and once LFO is delithiated, it never relithiates. The permanent lithium loss from LFO material shifts the LFO stoichiometry permanently from higher to lower values. This permanent shift in LFO stoichiometry leads to corresponding permanent OCP shifts from lower to higher OCP values. The second thing to note from Figure 2 is that after the 1st overcharge happens at around 4800 Ah cell throughput capacity, no parabolic profile for lithium release, unlike the one in the first 25 charge-discharge cycles, is observed during the future 25 normal charge-discharge cycles between each overcharge (the lithium moles stay unchanged and the profile of lithium release from LFO remains flat). This is because the permanent lithium loss from LFO during the first overcharge shifts its OCP close to 4.0 V, and now the upper normal charging voltage limit of 3.6 V is not enough to push more lithium moles out of LFO active material and when the cell is overcharged beyond 4.0 V, only then the more lithium would be released from LFO active material.

The third thing to note is that once the lithium moles in LFO start to deplete, the OCP of the LFO starts to saturate at higher values, and the size of the step-decrease in lithium moles during subsequent overcharges and the corresponding step-increase in OCP becomes lesser and lesser. This means that, as LFO depletes its lithium inventory, it becomes difficult for it to release further lithium moles and only fewer moles of lithium from LFO are released. In other words, the benefit of extra-lithium provided by LFO reduces slowly and if the faster lithium release is still desired, the overcharging cell voltage limits higher than 4.5 V and a longer CV hold period would be needed to achieve this. These observations made from Figure 2 justify the inferences and conclusions made in the first part of this section. Also, this section adds to the current theoretical knowledge about how sacrificing agents like LFO can be employed and made to work in commercial lithium-ion cells. Previous research (Johnson et al., 2010), (Su et al., 2016), (Liu et al., 2024) has mostly explored the use of lithium inventory from sacrificing agent either in one go (i.e. all lithium released during the first overcharge itself) or in the first few charge-discharge cycles. Adding to the current understating, we propose that the lithium release from additives can be more controlled and gradual so that

we can maximize the benefits of using them. A more detailed discussion on the controlled lithium release from LFO and the potential benefits is discussed in Section 3.

Also, reactions [1] and [2] (Liu et al., 2024) show that theoretically 4 moles of lithium-ions are released per mole of LFO (Li_5FeO_4), however, this simulation case suggests that the lithium release is more complex and is dependent on multiple interdependent operational and NE & PE (primary & secondary) parameters. To maintain the simplicity of work, only the effect of overcharging is discussed here. However, the PyBaMM simulation model developed in the work could be used to explore the effect of other parameters on lithium release from LFO.

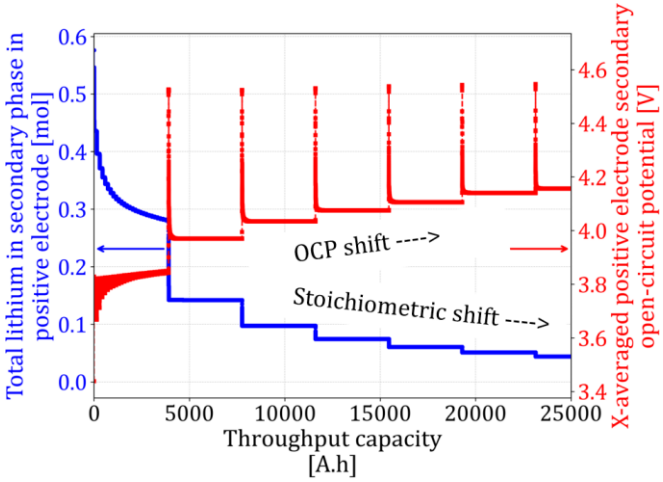

Figure 2: Simulation to show how lithium release & stoichiometric drift from LFO is connected to its OCP & OCP drift respectively.

Section 2: How does Lithium release from LFO affect SEI formation, lithium plating (instantaneous and dead lithium), and cell usable capacity?

This section explores the effect of the release of lithium inventory from LFO active material *('Total lithium in the secondary phase in PE [mol]')* with cell capacity throughput *('Throughput capacity [Ah]')*, using a PyBaMM Simulation Case 1, which is described in Section 1, on:

i. Lithiation of Graphite NE *('Total lithium in negative electrode [mol]')* and lithiation of the primary phase of PE i.e. LFP *('Total lithium in primary phase in positive electrode [mol]').* The results are shown in Figures 3(a) and 3(e).

ii. NE OCP *('X-averaged negative electrode open-circuit potential [V]')* and reaction overpotential *('X-averaged negative electrode reaction overpotential [V]').* Figure 3(b) shows the results for both potentials at NE.

iii. SEI formation *('Loss of lithium to negative SEI [mol]')*, instantaneous lithium plating *('Loss of lithium to negative lithium plating [mol]'),* conversion of instantaneously plated lithium to dead lithium *('Loss of lithium to negative dead lithium plating [mol]')* and total lithium loss because of side reactions such as SEI and dead lithium *('Total lithium lost to side reactions [mol]')* (O'Kane et al., 2022). Figures 3(c) and 3(d) show the results for all the above-mentioned sources of lithium losses.

iv. Cyclable lithium available for exchange between the NE and PE *('Total lithium in negative electrode [mol]'* and the corresponding *'Total lithium in primary phase in positive electrode [mol]')* and their effect on cell usable discharge capacity *('Discharge capacity [Ah]').* Figure 3(e) shows the cyclable lithium moles, and Figure 3(f) shows the usable discharge capacity of the cell.

To understand the impact of released lithium inventory from LFO active material, it is important to analyze all the results shown in Figures 3(a) to 3(f) in conjunction. Figure 3(a) shows that when the lithium moles from LFO are released into the cell (indicated by a decrease in *'Total lithium in the secondary phase in PE*

[mol]'), the over-lithiation of NE happens (marked by an increase in *'Total lithium in negative electrode [mol]'* from its reference value depicted by a dashed horizontal line in Figure 3(a)). The over-lithiation of NE pushes its OCP values close to zero and increases the reaction potential at the NE, the same has been observed in Figure 3(b). The increased reaction overpotential and OCP close to zero makes the NE unstable and accelerates SEI formation, instantaneously plated lithium and dead lithium (Sulzer et al., 2021), (MARQUIS, 2020), (O'Kane et al., 2022). The same is shown in Figures 3(c) and 3(d).

During overcharging, the moles of lithium released from LFO active material (indicated by a steep step-decrease in *'Total lithium in the secondary phase in PE [mol]')* increases the lithium inventory of the cell drastically. Newly Increased lithium inventory due to overcharging and resulting severe over-lithiation of NE, pushes its OCP, even more, closer to zero and increases the reaction overpotential even further making NE even more unstable. This leads to an increased loss of lithium moles to SEI formation, instantaneous plated lithium, and dead lithium. Note that the instantaneous plated lithium is not all dead lithium as some of the plated lithium gets stripped off in the subsequent discharge cycle and becomes part of cyclable lithium. This is also observed in Figure 3(c) where the decreasing trend of *'Loss of lithium to negative lithium plating [mol]'* is observed between two overcharge events. The conversion of instantaneously plated lithium to dead lithium is discussed in detail by (O'Kane et al., 2022) and is not the focus of the current study. Since the loss of lithium towards SEI and dead lithium is responsible for permanent lithium losses, the total loss in lithium inventory towards side reactions (*'Total lithium lost to side reactions [mol]')* is the sum of both of these losses and is shown in Figure 3(d). It is important to note that all the lithium moles that are released from the LFO material are not consumed by side reactions. For example, when the cell is cycled to reach a cell capacity throughput of 25000 Ah in Figure 3(d), the total lithium inventory lost to side reactions (*'Total lithium lost to side reactions [mol]')* is around 0.175 moles however the lithium inventory released from LFO (*'Total lithium in the secondary phase in PE [mol]')* is around 0.4 moles. Hence, LFO helps compensate for 0.175 moles, and the remaining 0.225 moles of lithium become part of the total cyclable lithium. This extra cyclable lithium gives rise to an increased usable cell capacity. The extra cyclable lithium also intercalates into the primary phase of PE *('Total lithium in primary phase in positive electrode [mol]')* during discharge and overlithiates it. Figures 3(e) show increased lithium moles in NE and the primary phase of PE indicating increased cyclable lithium moles, and Figure 3(f) shows the corresponding increase in usable discharge capacity of the cell.

.

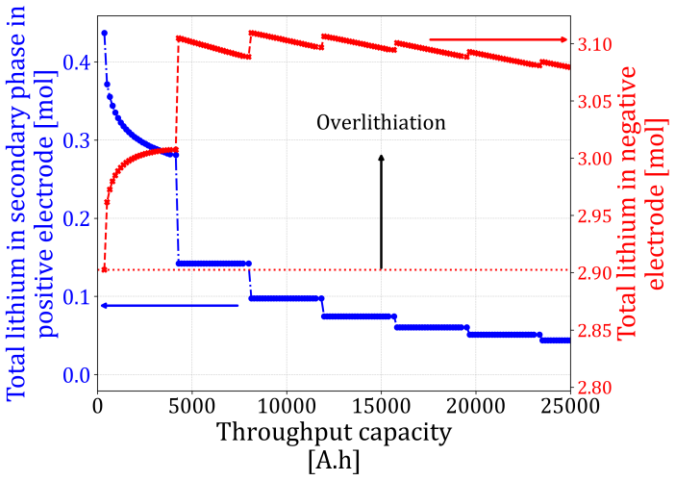

(a)

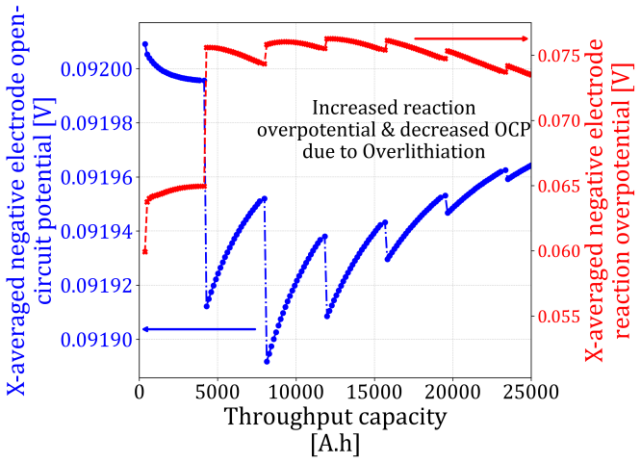

(b)

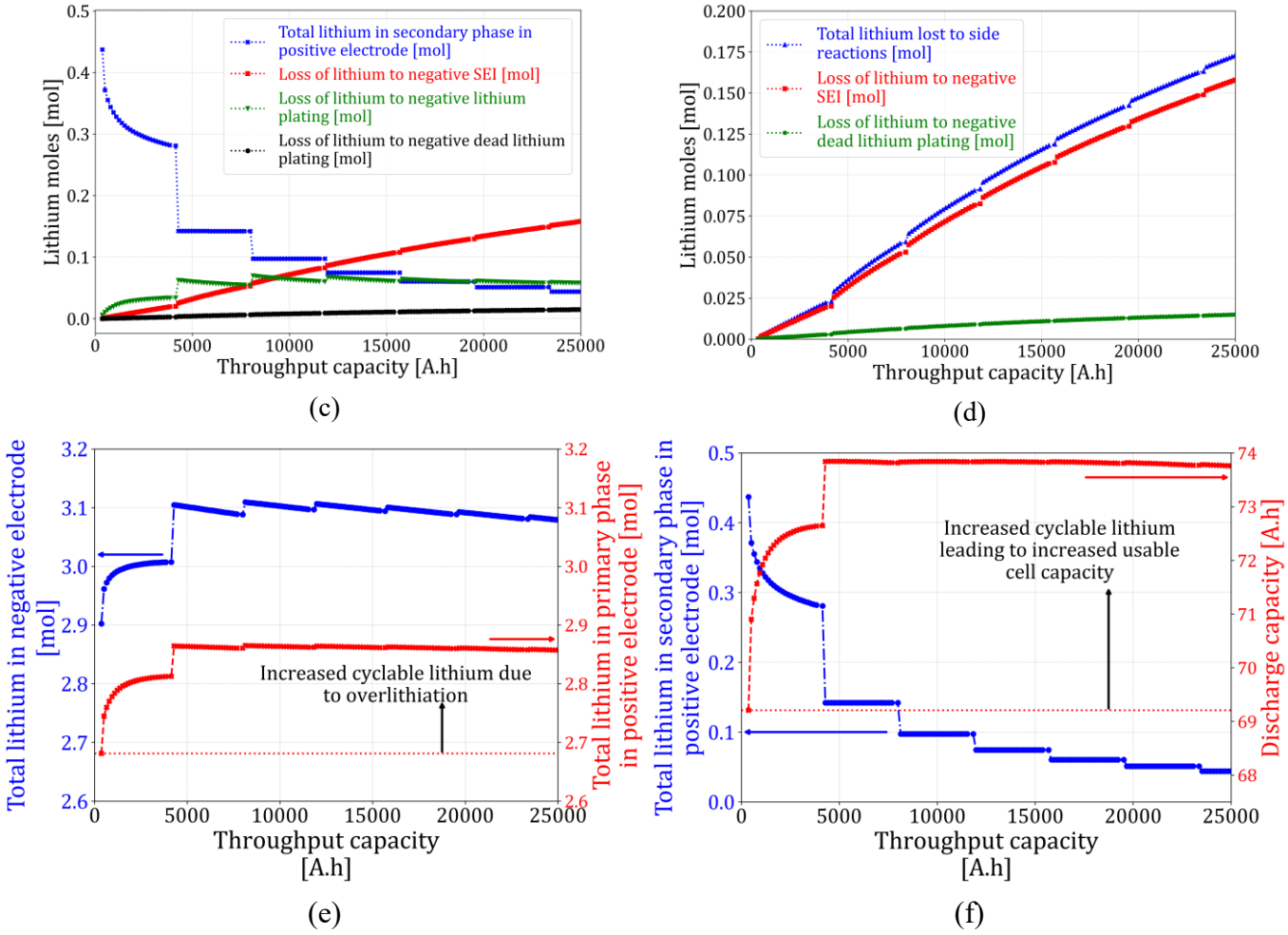

Figure 3:
(a) 'Total lithium in the secondary phase in PE [mol]' and 'Total lithium in negative electrode [mol]' vs 'Throughput capacity [Ah]'
(b) X-averaged negative electrode open-circuit potential [V]' and 'X-averaged negative electrode reaction overpotential [V]' vs 'Throughput capacity [Ah]'
(c) 'Total lithium in the secondary phase in PE [mol]', 'Loss of lithium to negative SEI [mol]', 'Loss of lithium to negative lithium plating [mol]' and 'Loss of lithium to negative dead lithium plating [mol]' vs 'Throughput capacity [Ah]'
(d) 'Total lithium lost to side reactions [mol]', 'Loss of lithium to negative SEI [mol]', and, 'Loss of lithium to negative dead lithium plating [mol]' vs 'Throughput capacity [Ah]'
(e) 'Total lithium in negative electrode [mol]', and 'Total lithium in primary phase in positive electrode [mol]'
(f) 'Total lithium in the secondary phase in PE [mol]', and 'Discharge capacity [Ah]' vs 'Throughput capacity [Ah]'

From the above discussion, one can conclude that:

1. It is also important to note that when LFO releases its lithium inventory faster (indicated by a steep decrease in lithium moles because of overcharging events), the SEI formation and lithium plating also increase suddenly. Also, as the cell in the early phase of its life is balanced with respect to the lithiation of NE and the primary phase of PE, the addition of extra lithium inventory overlithates these electrodes, leading to an unbalanced and unstable cell. Hence, it would be worthwhile to study the timing, i.e., when during the life of a cell the lithium is to be released from LFO to keep the cell in a balanced and stable state. Hence, it is extremely important to study the effect of timing (early or delayed) and frequency (slow or fast) of lithium release from the LFO on the lifetime of lithium-ion cells.
2. Increased lithium inventory because of LFO and the subsequent over-lithiation of NE favor the accelerated degradation of the lithium-ion cell as lithium loss to SEI and dead lithium plating increases

with increased lithium inventory. Therefore, total lithium inventory in the systems plays a crucial role in cell degradation and usable cell capacity. Since the amount of lithium inventory that can be released from LFO depends upon the weight/mass fraction of LFO used in the composite LFP-LFO cathode, hence it is important to understand the ideal weight fraction of LFO material in the composite LFP-LFO cathode-based lithium-ion cells which can give balance the cell degradation and provide longer cell life.

Section 3 explores the 4 different ways of controlling the timing & frequency of lithium release from LFO active material and their effect on cell life and Section 4 explores the various weight fractions of LFO content in composite LFP-LFO cathode and their effect on cell life.

Section 3: How to Control the time & frequency of lithium release from LFO active material and their effect on the cell life?

This section summarises the results for all four cases mentioned in Part 3 of the Methods section with 4% LFO weight fraction in composite LFP-LFO cathode. All these cases in principle control the time (early or delayed) & frequency (fast/frequent or slow/infrequent) of lithium release from LFO active material and their effect on the cycle life.

- ***Case1:*** Overcharge is done before every characterisation RPT (*Total 40 overcharges).* This represents the case of early & fast/frequent lithium release from LFO.
- ***Case2:*** Overcharge is done starting from 20^{th} characterisation RPT (i.e. delayed lithium release from LFO) and then done continuously till 40^{th} characterisation RPT (*Total 21 overcharges).* This represents the case of fast/frequent lithium release but starting only after cell throughput capacity equivalent to 500 aging cycles.
- ***Case3:*** Overcharge is done before 11^{th} characterisation RPT, 21^{st} characterisation RPT, 31^{st} characterisation RPT and 40^{th} characterisation RPT *(Total 4 overcharges only).* This represents the case of slow/infrequent & less lithium release from LFO.
- ***Case4:*** Overcharges is done continuously between 11^{th} to 21^{st} characterisation RPT and then 31^{st} to 40^{th} characterisation RPT (*Total 21 overcharges).* This represents the case of intermittent & fast/frequent lithium release from LFO.

Figures 4[a] and 4[b] show the comparison of the discharge capacity of a cell obtained from the RPT cycles and aging cycles with capacity throughput for all four cases. The discharge capacity of a cell obtained from the RPT cycles and aging cycles is also referred to as the cell's actual capacity and cell usable capacity respectively. The capacity throughput for each case corresponds to their respective equivalent 1000 (25 aging cycles per RPT * 40 RPTs) aging cycles. At BoL, the RPT discharge capacity of the cell is around 73.5 Ah, and the Aging cycle discharge capacity is around 69 Ah. Since the discharge C-rate of the RPT cycle is 0.2C and of the Aging cycle is 0.5C, the RPT cycle discharge capacity is higher than the Aging cycle. Also, as discussed in Section 2 above, the first controlled overcharge for the respective cases leads to increased cyclable lithium, which results in a rise in discharge capacity in the next corresponding immediate RPT cycle & aging cycles. From the plots, it is clear that RPT cycle discharge capacity and aging cycle discharge capacity are heavily dependent upon the cases of lithium release. Also, from Figure 4[b] we can conclude that Case 4 performs the best as it provides the highest mean aging cycle capacity or usable capacity. However, it is important to note that depending on the purpose where the lithium-ion cells are being used each case has the potential to perform better than the other. For example, Case1 provides higher useable capacity in the beginning phase of the cell life while Case2 provides the best useable capacity in the later half of cell life. Case3 is able to reserve the lithium inventory from LFO for much longer periods as only 4 overcharges are done and the reserved lithium inventory can be tapped whenever the user desires. More on lithium released from LFO for all four cases are discussed in Figure 5(d) below. Figure 5 below compares all four cases for (a) the loss of lithium to negative lithium plating, (b) the loss of lithium to negative SEI, (c) the average NE porosity (spatially averaged in x-direction) and (d) lithium release from secondary phase i.e. LFO in LFP-LFO composite cathode. Figure 5 shows that Case1 releases lithium from

LFO very early in the cell life, leading to unbalanced stoichiometries & very low OCP. This leads to accelerated lithium loss to SEI and faster porosity clogging. Case 2 & Case 3 shows least lithium loss to SEI & plating because the lithium release from LFO is delayed significantly which keeps the electrode stoichiometries in the balanced state. However, because of delayed and less lithium release from LFO, the full potential of LFO to provide more capacity is not utilised and hence these two cases don't perform well when usable discharge capacity from aging cycles is compared with case 1 & case 4. Case 4 is the most balanced case when judged on the basis of mean useable capacity and medium degradation rates until 1000 aging cycles.

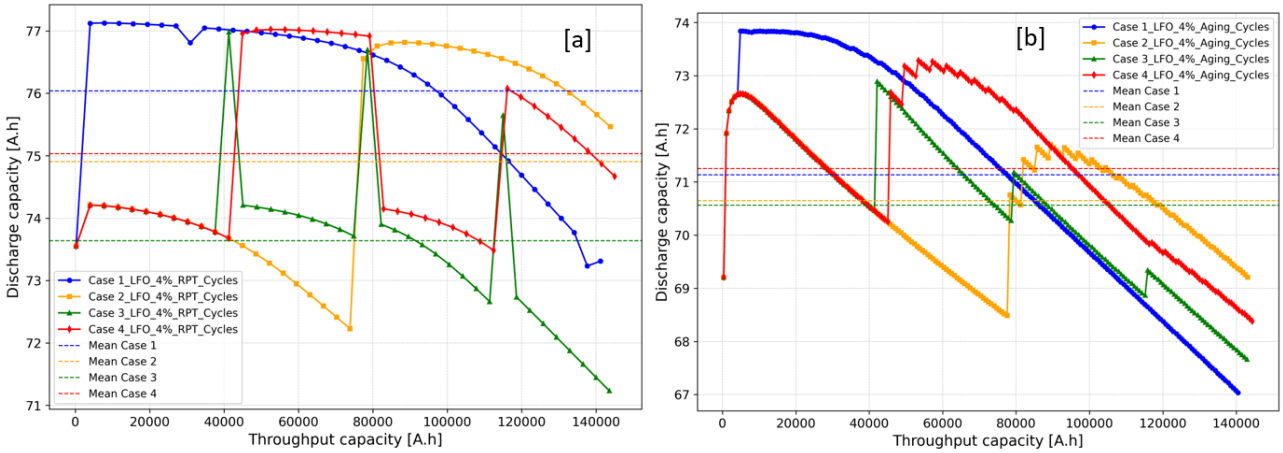

Figure 4: Comparison of Case 1, Case 2, Case 3 & Case 4 for Discharge Capacity obtained from: (a) RPT cycles (b) Aging cycles

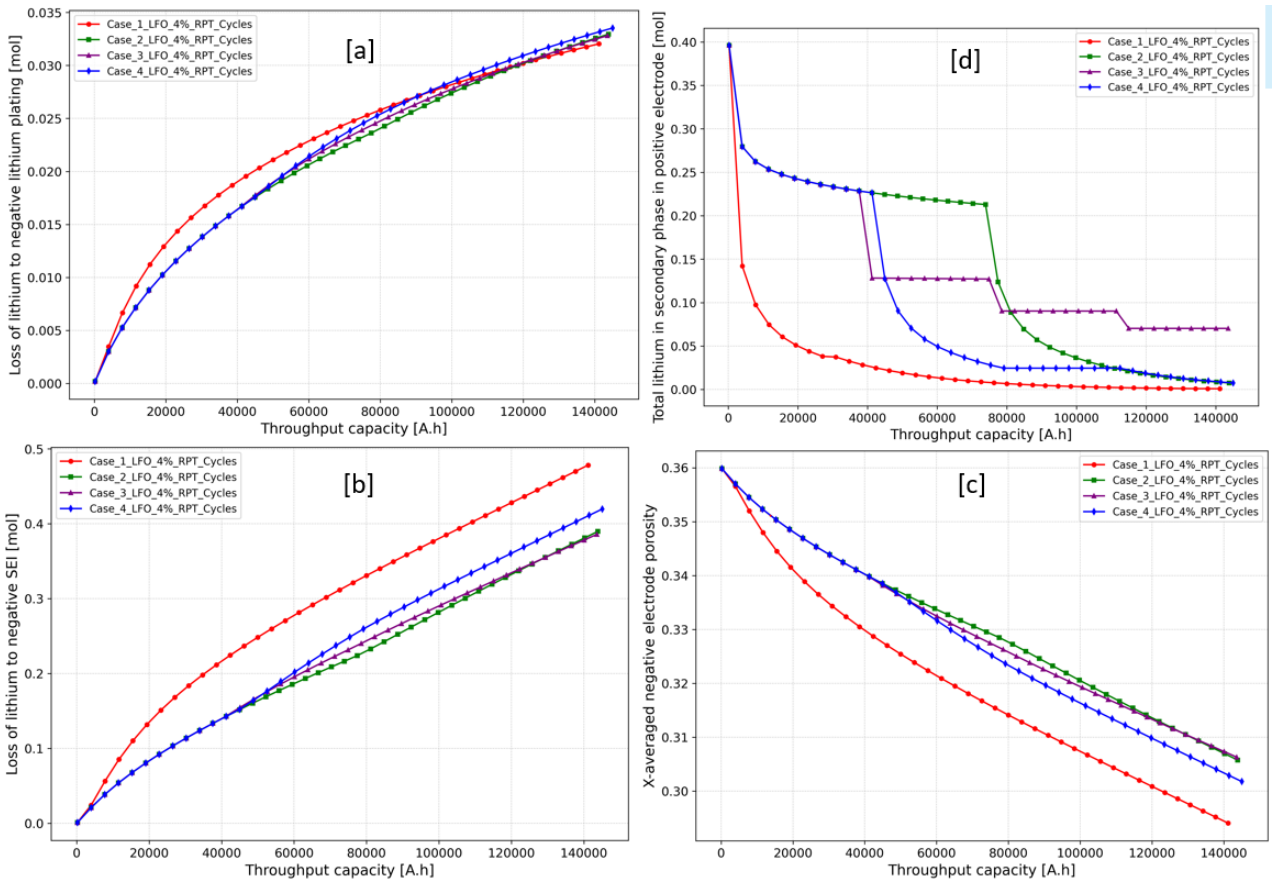

Figure 5: Comparison of Case 1, Case 2, Case 3 & Case 4 for (a) the loss of lithium to negative lithium plating, (b) the loss of lithium to negative SEI, (c) the average NE porosity (spatially averaged in the x-direction) and (d) lithium release from secondary phase i.e. LFO in LFP-LFO composite Cathode

Section 4: Effect of LFO weight fraction on the cell life

In the previous section, we observed that Case 4 performs the best when compared against the mean useable capacity and degradation rates. So, Case 4 is considered for its performance against the varying LFO weight fraction. Figure 6 compares the RPT & aging cycle discharge Capacity of case 4 for 0.1%, 1%, 4% & 10% weight fraction of LFO in composite LFP-LFO cathode. Figure 6 shows that when the LFO weight fraction is increased from 0.1% to 10%, discharge capacity obtained from RPT cycles as well aging cycle increases. But the benefit of increased capacity in the beginning is temporary and after the cell is degraded in consequent cycles, the case 4 with 10% LFO weight fraction shows drastic drop in discharge capacities.
As discussed previously in Section2, the drastic drop in discharge capacities is because the higher LFO weight fraction can release more lithium moles which keeps the cyclable lithium inventory as well as NE stoichiometries in the highly unbalanced state for longer time periods. This prolonged imbalance accelerates SEI formation and porosity clogging and eventually cell fail once the porosity of NE reaches close to zero, the same has been shown in Figure 7 which compares the loss of lithium to negative SEI and average NE porosity.

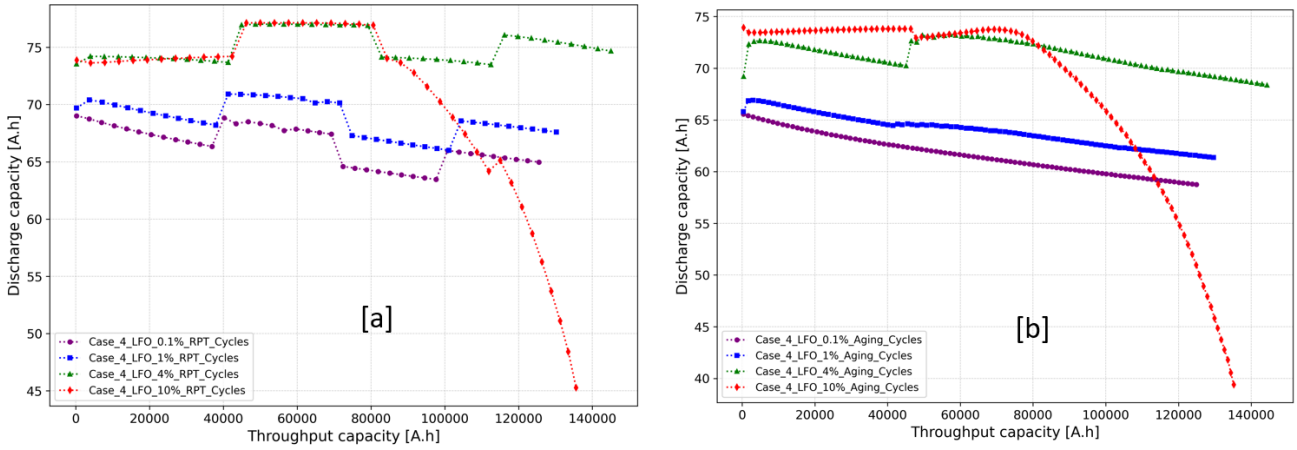

Figure 6: Comparison of 0.1%, 1%, 4% & 10% LFO weight fraction for case 4 discharge Capacity obtained from: (a) RPT cycles (b) Aging cycles.

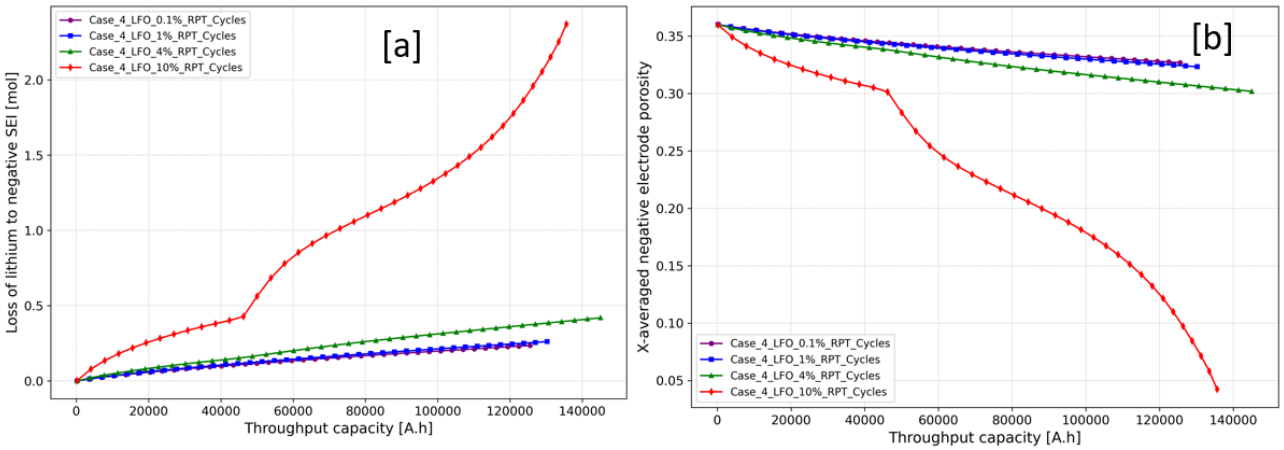

Figure 7: Comparison of 0.1%, 1%, 4% & 10% LFO weight fraction for case 4 (a) loss of lithium to negative SEI (b) the average NE porosity (spatially averaged in x-direction)

Conclusions

A full-cell physics-based model consisting of a composite LFP/LFO positive electrode (PE) and Graphite negative electrode (NE) is built in PyBaMM. The model considers SEI formation, lithium plating, and porosity clogging on NE. Model predictions show that the optimum weight fraction of LFO in LFP/LFO composite PE and an optimized method to control lithium release from LFO are crucial for minimizing cell degradation and achieving long-lasting, zero-degradation batteries. Controlled delayed & slow/infrequent lithium release maintains the cell balancing and reduces the degradation rates, while early & fast/frequent lithium release and excessive LFO content can accelerate the formation of SEI, lithium plating, and pore-clogging in the NE. Our findings also reveal that adding a higher LFO fraction appears beneficial in the beginning but is counterproductive as it promotes faster cell degradation resulting in a shorter cycle life of the cell. Hence this work concludes that achieving zero degradation requires not only just adding the lithium-rich additives to cell electrodes but also a suitable method to control lithium release, as well as an optimized weight fraction of additives. The results and conclusions from this work could be of direct relevance to cell designers and battery control engineers.

Methods

Part1: PyBaMM Model setup & model assumption

For setting the PyBaMM model, the standard Doyle-Fuller-Newman (DFN) model is set up using the model option highlighted in Figure 8. The details about all the model options can be found in PyBaMM documentation (PyBaMM, 2024).

For the simplicity of the model and not to deviate from the primary goal of showing the proof of concept for designing zero degradation battery, the following considerations are made in the model:

- ***Parameter Set:***
  - Beginning of Life (BoL) model for LFP is set using (Prada et al., 2013). The parameters used in degradation models are taken from (O'Kane et al., 2022).
- ***Degradation mechanisms:***
  - Only two degradation mechanisms (SEI & lithium plating) are considered at the NE.
  - The effect of porosity clogging due to both degradation mechanisms is also considered.
- ***Phases in Electrodes***
  - Single Phase in NE as only Graphite is used as the NE.
  - Two phases are Implemented in the PE of the cell (Primary phase-LFP, Secondary phase-LFO)
- ***Intercalation & De-intercalation Kinetics***
  - For NE: Butler-Volmer kinetics are considered as both Intercalation & De-intercalation kinetics is important here.
  - **For PE:**
    - Primary phase-LFP: Butler-Volmer kinetics are considered as both Intercalation & De-intercalation kinetics is important here.
    - Secondary phase-LFO: Tafel equation work for LFO is considered as LFO can only work one way (De-intercalation only).
- ***Hysteresis:*** The current sigmoid model is considered for LFP hysteresis, no hysteresis is considered for LFO as LFO works one way (De-intercalation only)

```
model_options = {
        SEI": ("interstitial-diffusion limited", "none"),
        "lithium plating": "partially reversible",
        "lithium plating porosity change": "true",
        "open-circuit potential": (("current sigmoid", "current sigmoid"), ("current sigmoid", "current sigmoid")),
        "SEI porosity change": "true",
        "intercalation kinetics": (("symmetric Butler-Volmer", "symmetric Butler-Volmer"), ("symmetric Butler-Volmer", "Tafel")),
        "particle phases": ("1", "2"),
    }
```

Figure 8: Snapshot of model options considered for setting the PyBaMM model

Part2: Setting up a virtual experiment in PyBaMM

The virtual experiment to simulate the long-term aging behavior of a full cell is shown in Figure 9. Charging during various steps is done by following the constant-current constant-voltage (CC-CV) charging protocol hereinafter referred to as charging. Discharge is always done using constant current. In summary, the virtual experimental protocol is divided into two parts:

1. Breaking cycle:
    a. The breaking cycle involved charging, followed by discharge and rest, and then charging again. This completes the breaking cycle. After the breaking cycle, the first rapid performance test (RPT0) is done to measure BoL discharge capacity. The breaking cycle happens only once.
2. Aging cycles
    a. Aging cycles involved the set of 25 cycles of charge-discharge-rest. They are represented by the constant 'N' in Figure 9. This set of 25 Aging cycles is followed by 1 normal *charging or overcharging cycle* and then a characterisation RPT. The set of 25 aging cycles, 1 normal charge or overcharge, and 1 characterisation RPT is then repeated 40 times to achieve 1000 aging cycles. The '40' repetitions of characterisation RPT are represented by the constant 'M' in Figure 9.
    b. The charge & discharge rates considered for aging cycles are fixed at 0.5C. The discharge rate for characterisation RPTs is considered as 0.2C.

RPT0 and the '40' repetitions of characterisation RPTs are hereinafter referred to as RPT cycles and are represented by the constant 'M' in Figure 9.

Other operation conditions:

- The charge & discharge rates considered for breaking cycles & aging cycles are fixed at 0.5C. The discharge rate for RPT cycles is considered as 0.2C.
- For normal charging, lower and upper cutoff voltage limits are considered as 2.5 V and 3.6 V respectively. CV hold at 3.6 V is considered until C/100
- For overcharging, lower and upper cutoff voltage limits are considered as 2.5 V and 4.5 V respectively. CV hold at 4.5 V is considered until C/100

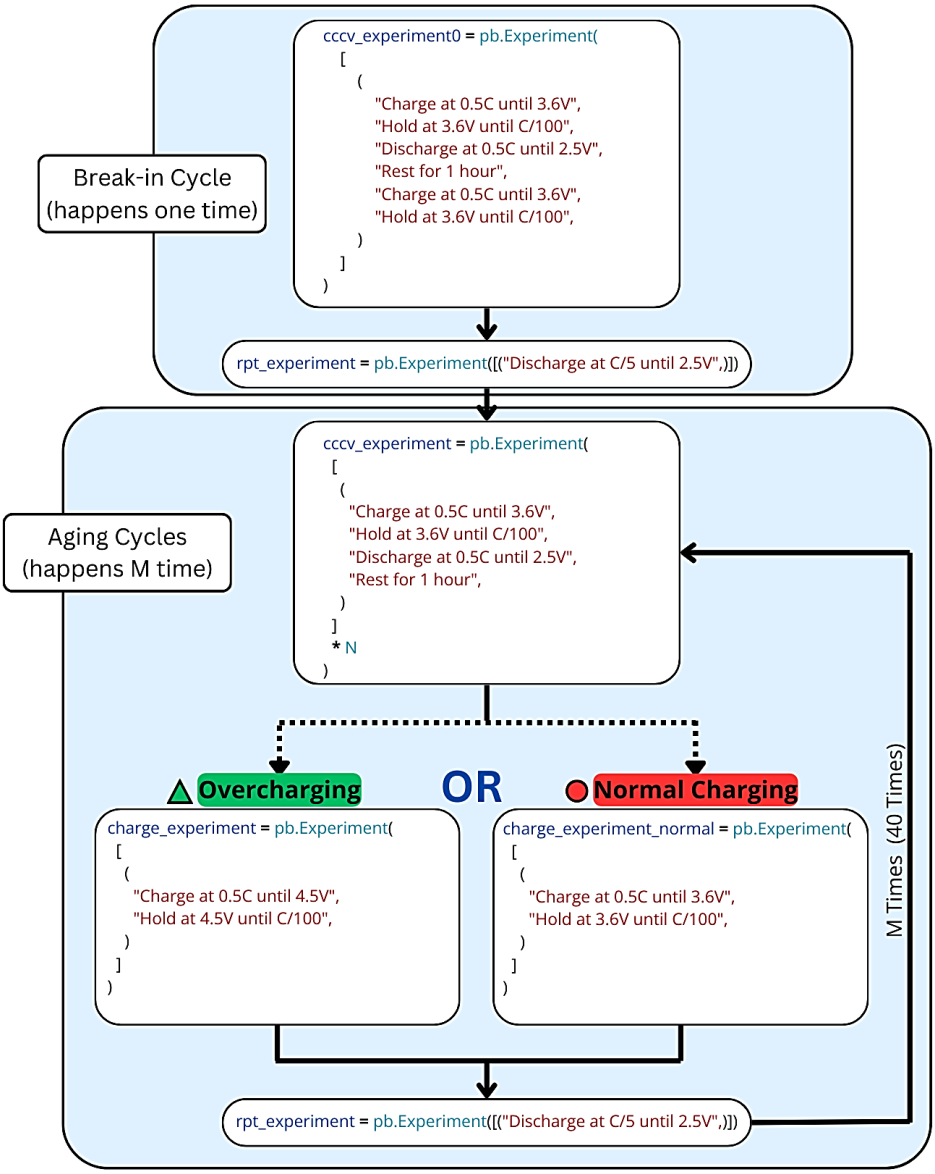

Figure 9: Snapshot of virtual experiment considered in the PyBaMM model

Part3: Setting up cases in PyBaMM

As explained in Part 2 of the Methods section above, the set of 25 aging cycles, *1 normal charge or overcharge,* and 1 characterisation RPT is repeated 40 times to achieve 1000 aging cycles. These 40 repetitions lead to 40 characterisation RPTs in total. So, based on the choice of performing either *normal charge or overcharge* before each characterisation RPT, different cases are defined. The cases are summarised below and the same has been depicted in Figure 10:

- ***Case1:*** Overcharges are done before every characterisation RPT. *Total 40 overcharges.*
- ***Case2:*** Overcharge are done starting from 20th characterisation RPT and then done continuously till 40th characterisation RPT. *Total 21 overcharges.*
- ***Case3:*** Overcharges are done before 11th characterisation RPT, 21st characterisation RPT, 31st characterisation RPT and 40th characterisation RPT. *Total 4 overcharges.*
- ***Case4:*** Overcharges are done continuously between 11th to 21st characterisation RPT and then 31st to 40th characterisation RPT. *Total 21 overcharges.*

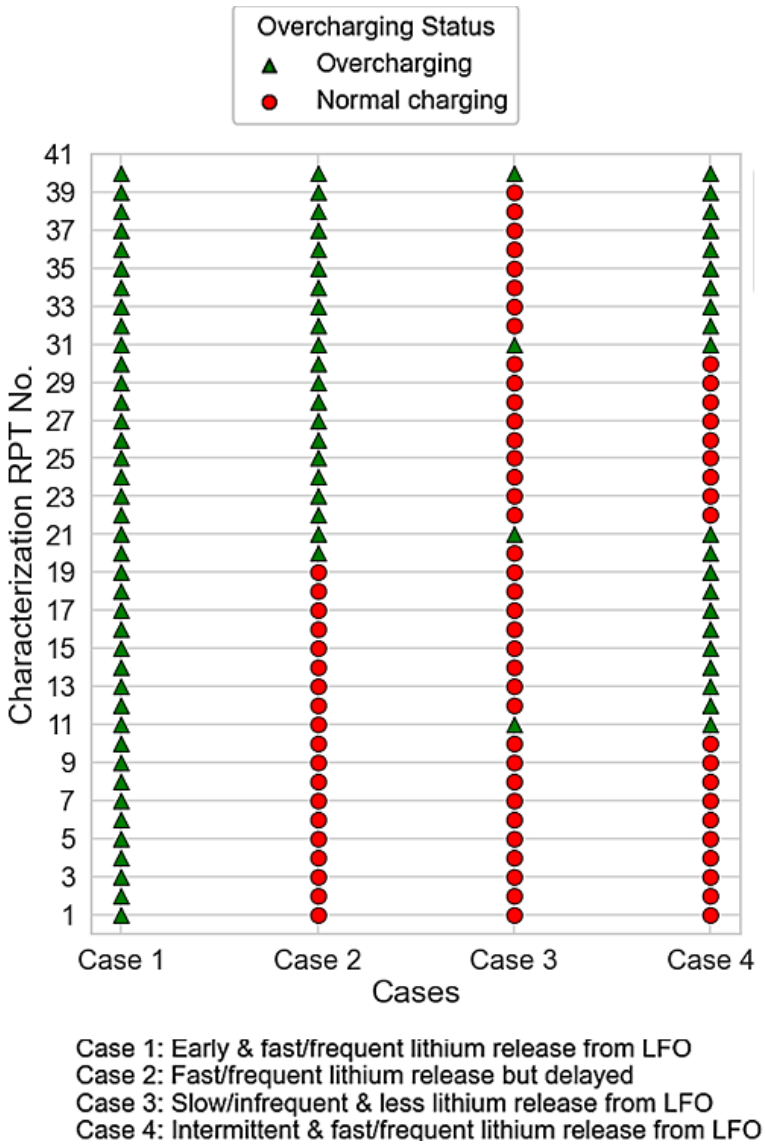

Figure 10: Snapshot of number of overcharging just before characterisation RPTs. Green triangle at a particular characterisation RPT number represent that overcharging is done just before that characterisation RPT and Red dot at a particular characterisation RPT number represent just the normal charging is done before that characterisation RPT.

References

[1] BIRKL, C. R., ROBERTS, M. R., MCTURK, E., BRUCE, P. G. & HOWEY, D. A. 2017. Degradation diagnostics for lithium ion cells. *Journal of Power Sources,* 341**,** 373-386.

[2] DOSE, W. M., MARONI, V. A., PIERNAS-MUÑOZ, M. J., TRASK, S. E., BLOOM, I. & JOHNSON, C. S. 2018. Assessment of Li-Inventory in Cycled Si-Graphite Anodes Using LiFePO4as a Diagnostic Cathode. *Journal of The Electrochemical Society,* 165**,** A2389-A2396.

[3] EDGE, J. S., O'KANE, S., PROSSER, R., KIRKALDY, N. D., PATEL, A. N., HALES, A., GHOSH, A., AI, W., CHEN, J., YANG, J., LI, S., PANG, M. C., BRAVO DIAZ, L., TOMASZEWSKA, A., MARZOOK, M. W., RADHAKRISHNAN, K. N., WANG, H., PATEL, Y., WU, B. & OFFER, G. J. 2021. Lithium ion battery degradation: what you need to know. *Phys Chem Chem Phys,* 23**,** 8200-8221.

[4] JOHNSON, C. S., KANG, S. H., VAUGHEY, J. T., POL, S. V., BALASUBRAMANIAN, M. & THACKERAY, M. M. 2010. Li2O Removal from Li5FeO4: A Cathode Precursor for Lithium-Ion Batteries. *Chemistry of Materials,* 22**,** 1263-1270.

[5] LIU, X., LIU, J., PENG, J., CAO, S., HU, H., CHEN, J., LEI, Y., TANG, Y. & WANG, X. 2024. Addressing the initial lithium loss of lithium ion batteries by introducing pre-lithiation reagent Li5FeO4/C in the cathode side. *Electrochimica Acta,* 481.

[6] MARQUIS, S. G. 2020. *Long-Term Degradation of Lithium-ion Batteries.* Doctor of Philosophy, University of Oxford.

[7] MURRAY, C. 2024. Rimac using pre-lithiation for 'zero capacity fade for first two years' in BESS. *Energy Storage News*.

[8] O'KANE, S. E. J., AI, W., MADABATTULA, G., ALONSO-ALVAREZ, D., TIMMS, R., SULZER, V., EDGE, J. S., WU, B., OFFER, G. J. & MARINESCU, M. 2022. Lithium-ion battery degradation: how to model it. *Physical Chemistry Chemical Physics,* 24**,** 7909-7922.

[9] PATHIRANA, T. 2024. *CATL's SECRET to "Zero" Degradation Batteries: Unveiling the Potential of LFO Cathode Additives* [Online]. Available: https://www.linkedin.com/pulse/catls-secret-zero-degradation-batteries-unveiling-lfo-pathirana-yfsuc/ [Accessed].

[10] PRADA, E., DI DOMENICO, D., CREFF, Y., BERNARD, J., SAUVANT-MOYNOT, V. & HUET, F. 2013. A Simplified Electrochemical and Thermal Aging Model of LiFePO4-Graphite Li-ion Batteries: Power and Capacity Fade Simulations. *Journal of The Electrochemical Society,* 160**,** A616-A628.

[11] SEPIDEH, A. 2017. *Lithium-Ion battery SOC estimation.* Doctor of Philosophy, University of Waterloo.

[12] SU, X., LIN, C., WANG, X., MARONI, V. A., REN, Y., JOHNSON, C. S. & LU, W. 2016. A new strategy to mitigate the initial capacity loss of lithium ion batteries. *Journal of Power Sources,* 324**,** 150-157.

[13] SULZER, V., MARQUIS, S. G., TIMMS, R., ROBINSON, M. & CHAPMAN, S. J. 2021. Python Battery Mathematical Modelling (PyBaMM). *Journal of Open Research Software,* 9.